

Gramian constraints in the joint inversion of airborne gravity gradiometry and magnetic data

Yue Zhu*, Michael S. Zhdanov and Martin Čuma, University of Utah and TechnoImaging

Summary

We apply Gramian constraints for the joint inversion of airborne gravity gradiometry and magnetic data. The method does not require any a priori knowledge about the types of relationships between the different model parameters, but instead determines the form of these relationships in the process of the inversion. The Gramian constraints make it possible to consider both linear and nonlinear relationships between the different physical parameters of a geological model. As an illustration, we consider in this paper polynomial relationships between different model parameters. The case study includes joint inversion of airborne gravity gradiometer (AGG) and magnetic data collected by Fugro Airborne Surveys in the area of McFaulds Lake located in northwestern Ontario. This case study demonstrates how joint inversion may enhance the produced subsurface images of a deposit.

Introduction

Zhdanov et al. (2012) have introduced a new approach to joint inversion of geophysical data using Gramian constraints, which are based on the minimization of the determinant of a Gram matrix of a system of different model parameters or their attributes (i.e., a Gramian). This approach does not require an a priori knowledge about the types of relationships between the different model parameters, but instead determines the form of these relationships in the process of the inversion. The Gramian constraints make it possible to consider both linear and nonlinear relationships between the different physical parameters of a geological model.

Principles of joint inversion using Gramian constraints

Consider forward geophysical problems for multiple geophysical data sets. These problems can be described by the operator relationships

$$d^{(i)} = A^{(i)}(m^{(i)}), i = 1, 2, 3, \dots, n; \quad (1)$$

where, in a general case, $A^{(i)}$ is a nonlinear operator, $d^{(i)}$ ($i = 1, 2, 3, \dots, n$) are different observed data sets (which may have different physical natures and/or parameters), and $m^{(i)}$ ($i = 1, 2, 3, \dots, n$) are the unknown sets of model parameters.

It is convenient to introduce the dimensionless weighted model parameters, $\tilde{m}^{(i)}$ defined as follows:

$$\tilde{m}^{(i)} = W_m^{(i)} m^{(i)}, \quad (2)$$

where $W_m^{(i)}$ is the corresponding linear operator of model weighting (Zhdanov, 2002).

The Gramian of a system of model parameters $\tilde{m}^{(1)}, \tilde{m}^{(2)}, \dots, \tilde{m}^{(n-1)}, \tilde{m}^{(n)}$ is introduced as a determinant, $G(\tilde{m}^{(1)}, \tilde{m}^{(2)}, \dots, \tilde{m}^{(n-1)}, \tilde{m}^{(n)})$, of the Gram matrix of a set of functions, $\tilde{m}^{(1)}, \tilde{m}^{(2)}, \dots, \tilde{m}^{(n-1)}, \tilde{m}^{(n)}$, according to the following formula:

$$G(\tilde{m}^{(1)}, \tilde{m}^{(2)}, \dots, \tilde{m}^{(n-1)}, \tilde{m}^{(n)}) = \begin{vmatrix} (\tilde{m}^{(1)}, \tilde{m}^{(1)}) & (\tilde{m}^{(1)}, \tilde{m}^{(2)}) & \dots & (\tilde{m}^{(1)}, \tilde{m}^{(n)}) \\ (\tilde{m}^{(2)}, \tilde{m}^{(1)}) & (\tilde{m}^{(2)}, \tilde{m}^{(2)}) & \dots & (\tilde{m}^{(2)}, \tilde{m}^{(n)}) \\ \dots & \dots & \dots & \dots \\ (\tilde{m}^{(n)}, \tilde{m}^{(1)}) & (\tilde{m}^{(n)}, \tilde{m}^{(2)}) & \dots & (\tilde{m}^{(n)}, \tilde{m}^{(n)}) \end{vmatrix} \quad (3)$$

It is shown in Zhdanov et al., (2012) that the Gramian provides a measure of correlation between the different model parameters or their attributes. By imposing the additional requirement of the minimum of the Gramian in regularized inversion, we obtain multimodal inverse solutions with enhanced correlations between the different model parameters or their attributes.

For a regularized solution of the inverse problem, we introduce a parametric functional with the Gramian stabilizers,

$$P(\alpha)(\tilde{m}^{(1)}, \tilde{m}^{(2)}, \dots, \tilde{m}^{(n)}) = \sum_{i=1}^n \|\tilde{A}^{(i)}(\tilde{m}^{(i)}) - \tilde{d}^{(i)}\|_D^2 + \alpha c_1 \sum_{i=1}^n S_{MN,MS,MGS}^{(i)} + \alpha c_2 \sum_{i=1}^n G(\tilde{m}^{(1)}, \dots, \tilde{m}^{(n)}), \quad (4)$$

where $\tilde{A}^{(i)}(\tilde{m}^{(i)})$ are the weighted predicted data,

$$\tilde{A}^{(i)}(\tilde{m}^{(i)}) = W_d^{(i)} A^{(i)}(\tilde{m}^{(i)}),$$

α is the regularization parameter, and c_1 and c_2 are the weighting coefficients determining the weights of the different stabilizers in the parametric functional.

The terms $S_{MN}^{(i)}$, $S_{MS}^{(i)}$, and $S_{MGS}^{(i)}$ are the stabilizing functionals, based on minimum norm, minimum support, and minimum gradient support constraints, respectively (Zhdanov, 2009). The solution of the minimization problem for the parametric functional (4) with the Gramian stabilizers can be achieved by using the re-weighted conjugate gradient method, as discussed in Zhdanov et al., (2012).

Joint inversion of potential fields using Gramian constraints

We should note that the Gramian could be used to enhance both the linear and nonlinear relationships between different model parameters as well. For example, in a case of joint inversion of the gravity and magnetic data, we consider two different model parameters: anomalous density, $\Delta\rho$ and magnetic susceptibility, χ . We can introduce the auxiliary model parameters, $m^{(i)}$ ($i = 1, 2, 3, \dots, n$), as follows:

$$m^{(1)} = \Delta\rho; m^{(2)} = \Delta\rho^2; \dots m^{(n-1)} = \Delta\rho^{(n-1)}; m^{(n)} = \chi.$$

In this case, the minimization of the Gramian will result in enforcing the polynomial relationship between magnetic susceptibility, χ , and anomalous density:

$$\chi = a_1\Delta\rho + a_2\Delta\rho^2 + \dots + a_{n-1}\Delta\rho^{(n-1)}. \quad (5)$$

It is important to note that we do not need to know the specific values of the coefficients a_1, a_2, \dots, a_{n-1} of this relationship in order to apply the joint inversion.

Model study

We have evaluated numerous models with various density and susceptibility relationships. Here we present a model that has quadratic dependence between the density and susceptibility as follows:

$$\chi = 0.13\rho^2 + 0.26\rho.$$

The gravity field and gravity gradient components, $g_z, g_{xx}, g_{yy}, g_{zz}$, and TMI components were simulated for this model and used in the inversion. Figure 1 shows the vertical cross sections of this synthetic model.

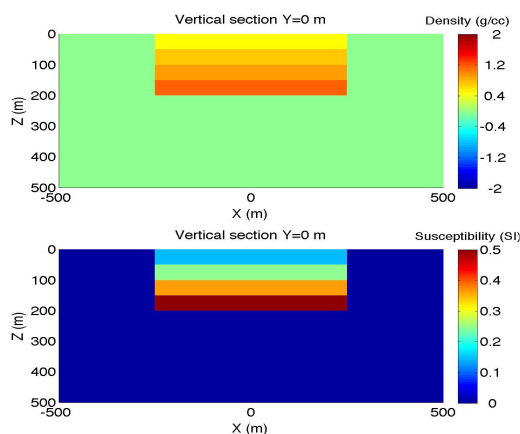


Figure 1: Vertical cross sections of the anomalous density (top) and susceptibility (bottom) distribution of the synthetic model.

In order to recover the quadratic relationship between the two model properties, a Gramian constraint with three model parameters was used:

$$S_G = \begin{vmatrix} (\tilde{m}^{(1)}, \tilde{m}^{(1)}) & (\tilde{m}^{(1)}, \tilde{m}^{(2)}) & (\tilde{m}^{(1)}, \tilde{m}^{(3)}) \\ (\tilde{m}^{(2)}, \tilde{m}^{(1)}) & (\tilde{m}^{(2)}, \tilde{m}^{(2)}) & (\tilde{m}^{(2)}, \tilde{m}^{(3)}) \\ (\tilde{m}^{(3)}, \tilde{m}^{(1)}) & (\tilde{m}^{(3)}, \tilde{m}^{(2)}) & (\tilde{m}^{(3)}, \tilde{m}^{(3)}) \end{vmatrix},$$

where $\tilde{m}^{(1)} = \mathbf{W}_{m^{(1)}}\Delta\rho$, $\tilde{m}^{(2)} = \mathbf{W}_{m^{(2)}}\chi$ and $\tilde{m}^{(3)} = \mathbf{W}_{m^{(3)}}\Delta\rho^2$.

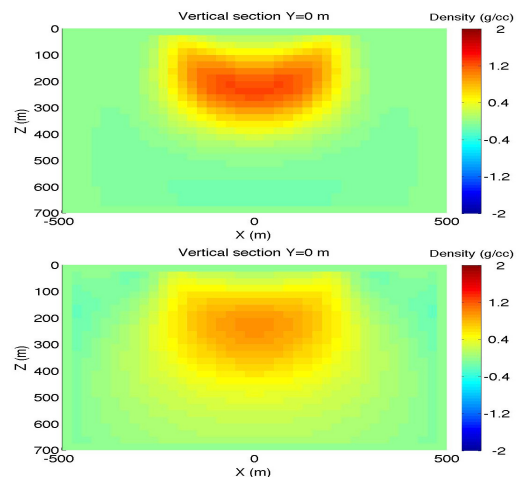


Figure 2: Vertical cross sections of the anomalous density distribution by the joint (top) and the independent (bottom) gravity inversions.

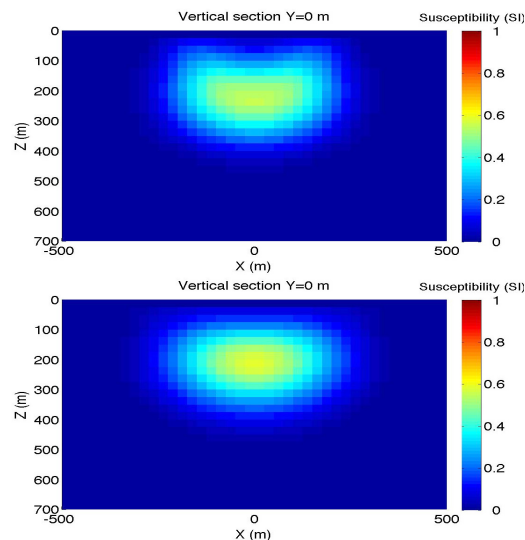


Figure 3: Vertical cross sections of the predicted susceptibility distribution by the joint (top) and the independent (bottom) magnetic inversions.

Figures 2 and 3 show cross sections of the independent and

Joint inversion of potential fields using Gramian constraints

joint inversion result. The joint inversion helps get a more compact density distribution of the predicted model. Cross plot of density vs. susceptibility in Figure 4 reveals the advantage of using the Gramian constraint in the joint inversion. The joint inversion recovers the quadratic relationship between density and susceptibility, which agrees very well with the synthetic curve.

Finally, we would like to note that in practice we do not know a priori what specific relationships may exist between the different model parameters. The use of the Gramian constraints with a more general relationship in the stabilizer makes it possible to answer this question based only on the observed data.

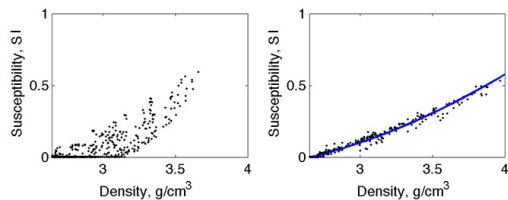


Figure 4: Cross plots of the density versus susceptibility. The plot for the model computed by the independent inversions is on the left. The one computed by the joint inversion is on the right. The blue curve indicates the synthetic quadratic relationship between density and susceptibility.

Case study: inversion of the airborne geophysical data in McFaulds Lake, Ontario

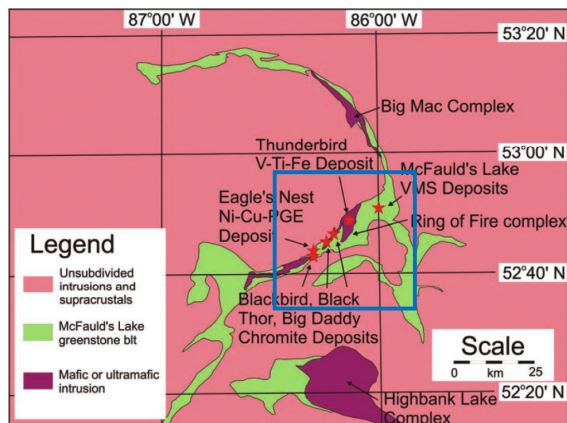


Figure 5: Geological sketch map with known mineralization in the Ring of Fire region (from Mungall et al., 2010). Blue box delineates the case study area.

McFaulds Lake is located in the northwestern Ontario. It is the host to the “Ring of fire,” which is a roughly north-south trending Archean greenstone belt (Figure 5). This westward-concave belt sits on the west edge of the James

Bay Lowland in far northwestern Ontario and is currently a focus of major mining explorations. Various economic mineral deposit types are known to exist in this area, including magmatic Ni-Cu-PGE, V-Ti-Fe and chromite mineralization, volcanic massive sulfide (VMS) mineralization and diamonds hosted by kimberlite.

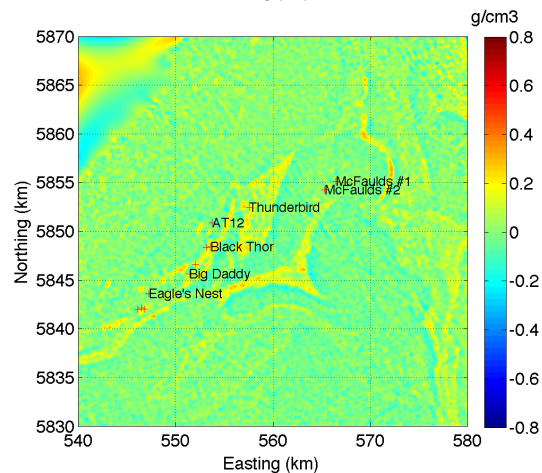
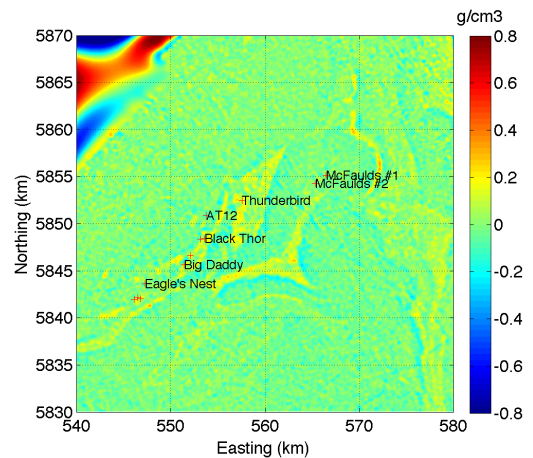


Figure 6: Horizontal cross sections of density obtained with independent FTG (top) and joint (bottom) inversions.

Airborne geophysical survey was carried out in the McFaulds Lake region by Fugro between 2010 and 2011 collecting airborne gravity gradiometry (AGG) and magnetic data. This project was collaboratively operated between the Ontario Geological Survey (OGS) and the Geological Survey of Canada (GSC).

In this case study, we focused on a subset of the AGG and magnetic data covering the southern part of the greenstone belt (Figure 5). The deposit resolution inversion domain

Joint inversion of potential fields using Gramian constraints

covered area of $40 \times 40 \text{ km}^2$ to 2 km depth and 50 m^3 cells, resulting in roughly 34 million cells and 1,080,000 data points. We used all the six provided AGG components and TMI and inverted for density and susceptibility. Both physical properties converged well, reaching 6% and 3% L2 norm misfit, respectively, after 100 iterations, which took 16 hours on four cluster nodes using 2 GPUs per node.

In previous synthetic studies, we found that the joint inversion algorithm with the quadratic Gramian constraint is capable of recovering both the linear and quadratic relationships between the anomalous density and susceptibility. We use the quadratic relationship constraint to invert the data jointly.

Figures 6 and 7 show the horizontal cross sections of the recovered density and susceptibility models using independent and joint inversions. Note that, while the susceptibility images are fairly similar, the density image is more compact. The chromite (Black Thor, Big Daddy), ferric (Thunderbird) and nickel (Eagle's Nest) deposits show a distinct correlated density and susceptibility anomaly within a specific area selected for the inversion. The McFaulds VMS deposits do not have strong gravity or magnetic response. The inverted volume also shows several other strong gravity and magnetic sources that are not yet associated with known deposits.

Conclusions

The interpretation of geology from geophysical data represents a data fusion problem, as different geophysical fields provide information about different physical properties of the earth. In many cases, the various geophysical data are complementary and self-constraining, making it natural to consider their joint inversion based on the correlation between different physical properties of the rocks. By using Gramian constraints, we are able to invert jointly multimodal geophysical data by enforcing the correlations between different model parameters or their attributes (e.g., spatial gradients). Importantly, the method assumes that a correlation between the different model parameters or their attributes exists, but the specific forms are unknown. In addition, the Gramian could be used to enhance the nonlinear relationships between different model parameters as well. Our case study for joint inversion of gravity gradiometry and magnetic data from McFaulds Lake, Ontario, demonstrates how the joint inversion may enhance the produced subsurface images of a deposit.

Acknowledgments

The authors acknowledge support from the University of Utah's Consortium for Electromagnetic Modeling and Inversion (CEMI). The authors acknowledge also TechnoImaging and the Ontario Geological Survey (OGS) and the Geological Survey of Canada (GSC) for support of this research and permission to publish.

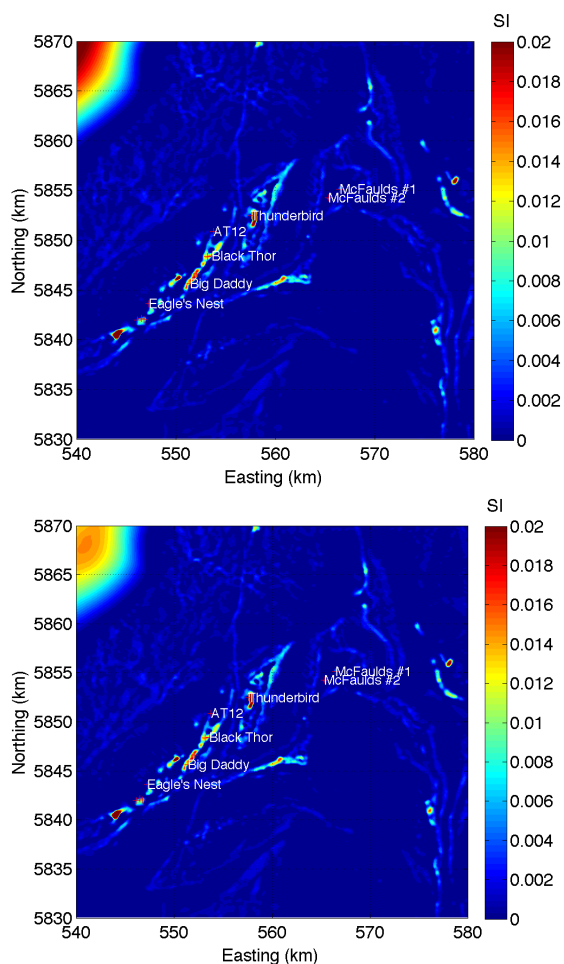


Figure 7: Horizontal cross sections of susceptibility obtained with independent TMI (top) and joint (bottom) inversions.

<http://dx.doi.org/10.1190/segam2013-0735.1>

EDITED REFERENCES

Note: This reference list is a copy-edited version of the reference list submitted by the author. Reference lists for the 2013 SEG Technical Program Expanded Abstracts have been copy edited so that references provided with the online metadata for each paper will achieve a high degree of linking to cited sources that appear on the Web.

REFERENCES

- Balch, S. J., J. Mungall, and J. Niemi, 2010, Present and future geophysical methods for Ni-Cu-PGE Exploration: Lessons from McFaulds Lake, Northern Ontario: Society of Economic Geologists: Special Publication, **15**, 559–572.
- Mungall, J. E., J. D. Harvey, S. J. Balch, B. Azar, J. Atkinson, and M. A. Hamilton, 2010, Eagle's nest: A magmatic Ni-sulfide deposit in the James Bay Lowlands, Ontario, Canada: Society of Economic Geologists: Special Publication, **15**, 539–557.
- Ontario Geological Survey and Geological Survey of Canada, 2011, Ontario airborne geophysical surveys, gravity gradiometer and magnetic data, grid, and profile data (ASCII and Geosoft® formats) and vector data, McFaulds Lake area: Ontario Geological Survey, Geophysical Data Set 1068.
- Zhdanov, M. S., 2002, Geophysical inverse theory and regularization problems: Elsevier.
- Zhdanov, M. S., 2009, New advances in regularized inversion of gravity and electromagnetic data: Geophysical Prospecting, **57**, 463–478, doi: 10.1111/j.1365-2478.2008.00763.x.
- Zhdanov, M. S., A. V. Gribenko, and G. A. Wilson, 2012, Generalized joint inversion of multimodal geophysical data using Gramian constraints: Geophysical Research Letters, **39**, no. 9, L09301, <http://dx.doi.org/10.1029/2012GL051233>.